5th International Conference on Biaxial/Multiaxial Fatigue and Fracture
Cracow'97, Poland

Takashi OGATA* and Yukio TAKAHASHI*

Development of a High-Temperature Biaxial Fatigue Testing Machine Using a Cruciform Specimen

Central Research Institute of Electric Power Industry

keywords: Biaxial fatigue, Cruciform specimen, high-temperature, fractography, life prediction

ABSTRACT: *In order to perform high-temperature fatigue tests under a wide range of biaxial stress state, a high-temperature biaxial fatigue testing machine, which can apply equibiaxial tension and compression loading to a cruciform specimen, was developed. Strain controlled biaxial fatigue tests on the 316FR stainless steel were performed under proportional and nonproportional loading, in the latter of which 90° phase difference existed between x and y directional strain, at 550°C. Through comparison of the load-strain data between x and y direction obtained from the equibiaxial tests, it was confirmed that the biaxal fatigue tests were successfully performed by using the new developed machine. Fatigue failure lives did not correlated well with Mises equivalent strain range, giving the shortest life for the nonproportional loading. Based on the experimental results represented on the εx-εy diagram, a new biaxial fatigue criterion, equivalent normal strain range Δεu, was proposed. Biaxial fatigue lives correlated well with Δεu regardless of the strain ratio and the loading mode.*

Introduction

Majority of high-temperature structures and components in power plants are subjected to biaxial/multiaxial fatigue loading depending on their configurations and operating conditions. Therefore establishment of a biaxial/multiaxial fatigue life criterion is important for design and remaining life assessment of actual components to maintain reliable operation. The authors have been performing tension/compression and torsion tests under proportional and nonproportional loading conditions at high-temperature and elucidated fatigue failure mechanism and life property under biaxial loading(1)-(3). However a whole range of biaxial strain state is not covered by the tension-torsion loading. A biaxial fatigue test using a cruciform specimen is able to cover whole strain state ranging from torsion to equibiaxial. Although such a testing machine can be thus effectively used for thestudy on biaxial fatigue, very limited data is available(4), (5) due to technological difficulty, especially at high-temperature.

In this study, a new high-temperature biaxial fatigue testing machine using a cruciform speci-

men is developed and biaxial fatigue tests on 316 stainless steel are performed under proportional and nonproportional loading conditions at 550°C. Cyclic deformation and failure characteristics under biaxial fatigue loading are described, and a new biaxial fatigue criterion is proposed based on the experimental results.

Development of a high-temperature biaxial fatigue testing machine

Based detailed specification of a high-temperature in-plane biaxial fatigue testing machine (HTBFM) provided by CRIEPI, the machine was manufactured and installed by MTS Corporation. An outline of the newly developed HBFM is addressed in this section.

Loading and heating equipment

Appearance of a main frame of the HBFM with a heating device and a controller is shown in Fig.1. The HTBFM consists of four hydraulic servo driven actuators and wedge grips mounted in a rigid load frame which can maintain high stiffness of the system. Tensile and compressive loads can be applied by two pairs of actuators independently and controlled by digital control system. The maximum applied load is 100kN. Load ratio and phase correlation can be arbitrarily chosen. To mount a cruciform specimen, two actuators in x direction and one actuator in y direction have L shape plates to determine the specimen position on the grips which allow to mount the specimen easy. In order to maintain specimen center at a fixed position, the controller adopted the Control Matrix concept which allows each control loop to be stabilized and optimized. Specimen center is able to be maintained by minimizing the differentiation of the LVDT signal between two actuators in the same axis independently from another axis. Concept of center control is shown in Fig.2. Movement of the point of specimen center is less than 2μm during cyclic test with strain range of 1%. The specimen can be heated up to 1000°C by the induction heating device with a heating coil. Temperature distribution at the control temperature of 550°C is ranging from 548°C to 553°C within the gage area (15mm diameter in the center of the specimen) .

Specimen design and strain measurement

Important things to consider in the design of a cruciform specimen are to provide uniform stress strain field in the center of the specimen and to avoid crack initiation at outside of gage

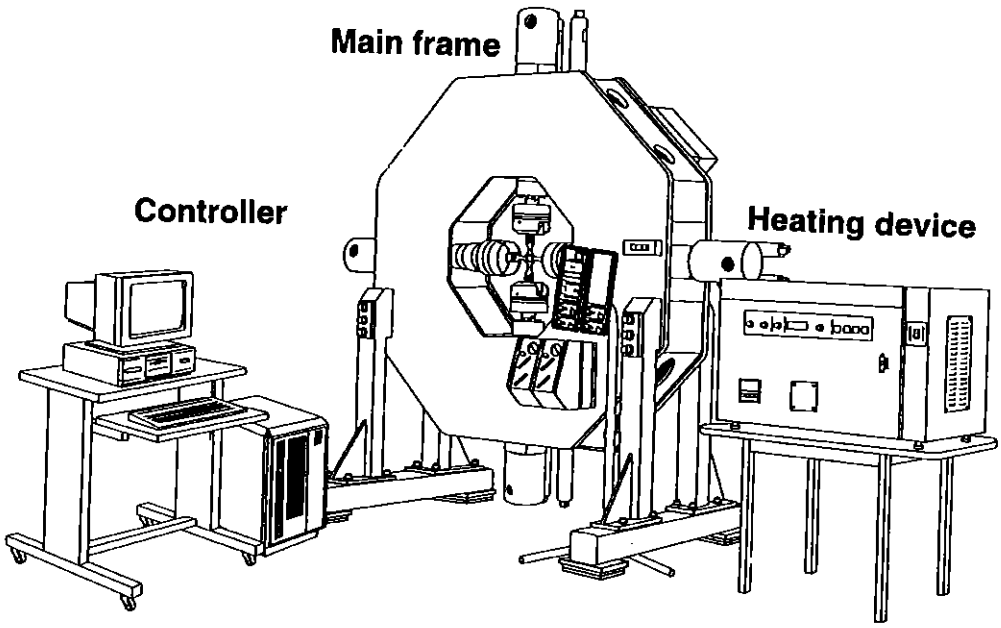

Fig.1 Appearance of biaxial fatigue testing machine

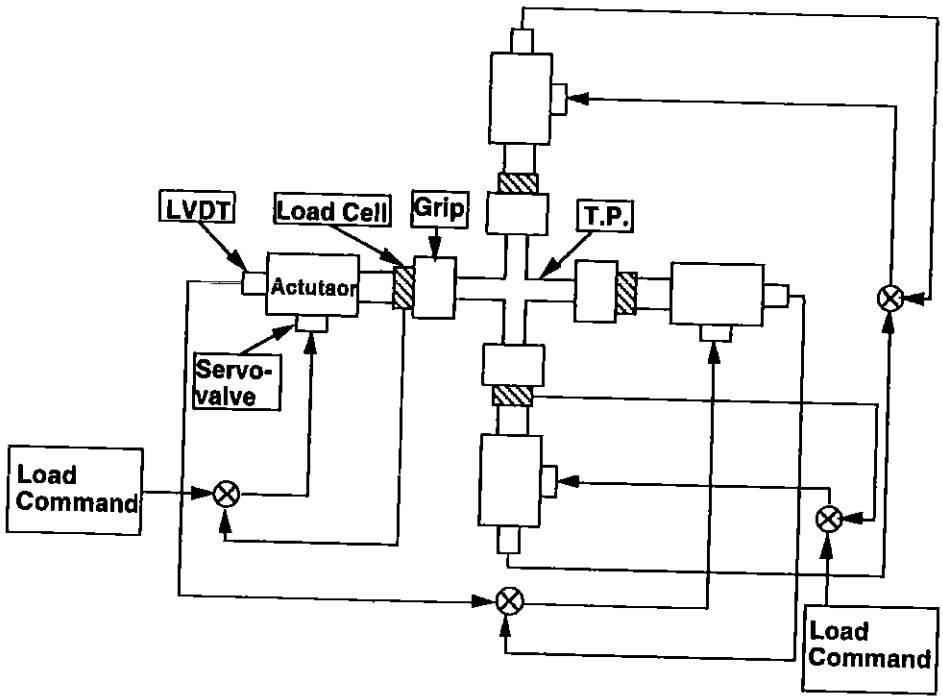

Fig.2 Concept of load contorol testing

area due to unpreferable stress concentration. The basic geometry was determined referring to the study by Sakane and Ohnami(4). The specimen geometry was designed by a 3-D elastic-plastic finite element analysis using the Marc K6 with a 3D 8 nodes-cubic element. Some improvements were made from pre- determined geometry to increase specimen stiffness and decrease stress concentration at specimen shoulders. Final specimen geometry is shown in Fig.3. The specimen has 2.5mm thickness with 15mm diameter gage area in the center and shoulders with smooth curvature of 25mm radius. Elastic-plastic stress analysis results under equibiaxial loading condition represented by von Mises stress are shown in Fig.4. It is seen that almost uniform stress field could be obtained in the gage area and unpreferable stress concentration at outside of gage area did not occur.

A high-temperature biaxial extensometer(HBE) applied for the cruciform specimen to control x and y directional strains was also developed. The HBE was manufactured by combining two separate uniaxial extensometers into one structure. The x and y directional strains can be controlled independently. Measured noise level at a cyclic condition was lower than 30mV and interference level by movement of other axis was lower than 0.003%.

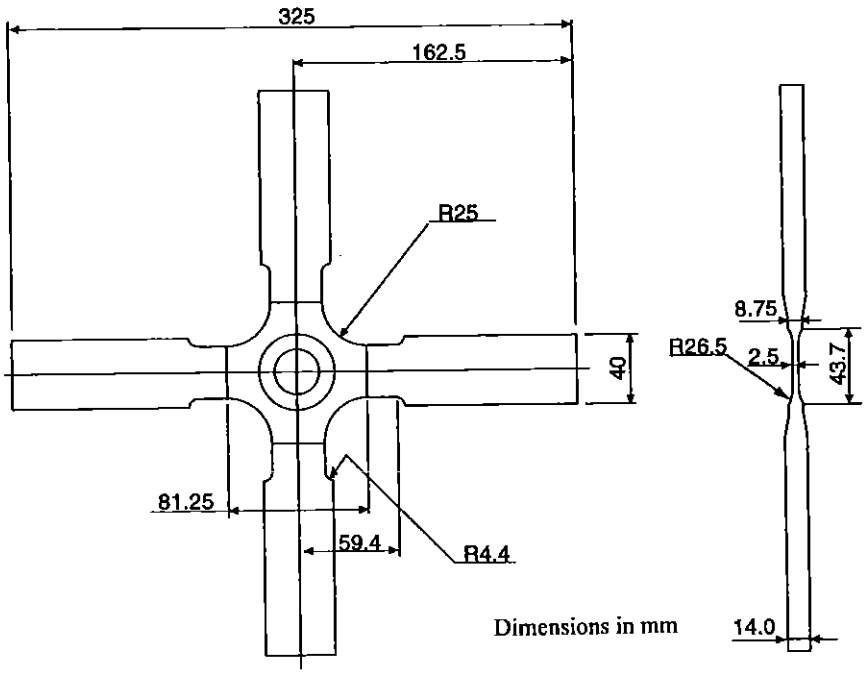

Fig.3 Cruciform specimen geometry

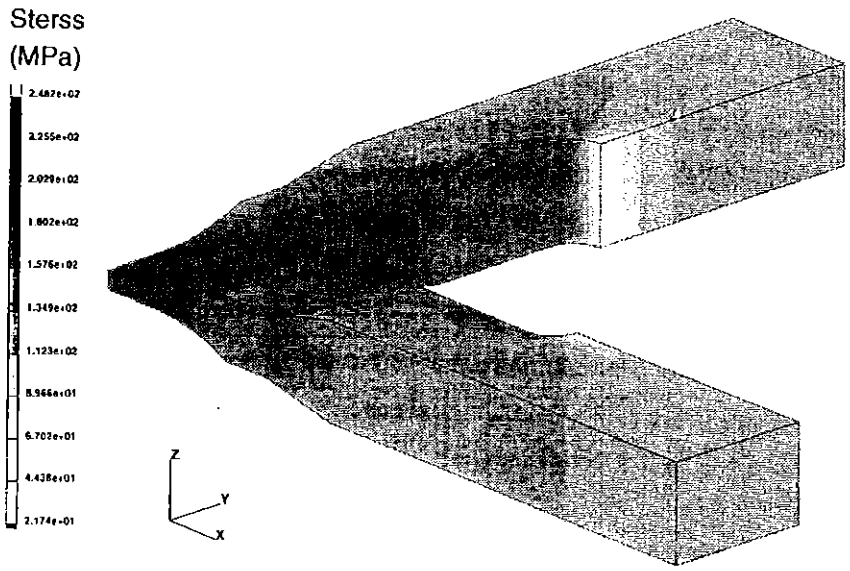

(a) Misces equivalent stress distribution

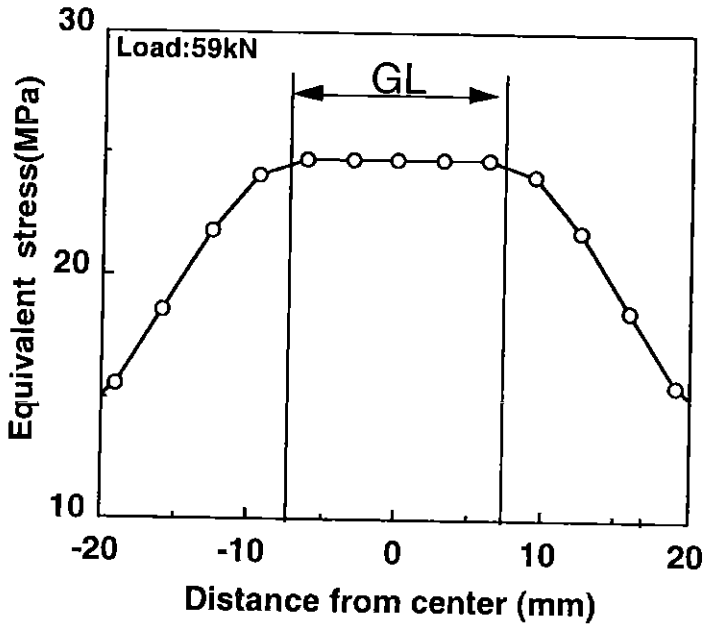

(b) Stress distribution aroud gage regime

Fig.4 Elastic-plastic Stress analysis results of the cruciform specimen

Experimental Procedure

A material used in this study was 316 stainless steel specially improved as a fast breeder component material (316FR). Chemical composition is shown in the table1. The feature of chemical composition of this material is medium nitrogen and low carbon contents which suppress grainboundary degradation caused by precipitation of chromium carbides. The cruciform specimen shown in Fig.3 was machined from a hot rolled plate with 50mm thickness.

Strain controlled fatigue tests were performed at 550°C under the test conditions shown in Fig.5. In the proportional loading tests, surface principal strain ratio, ϕ was defined as the ratio of x directional strain, ε_x to y directional strain, ε_y applied to the specimen. ϕ = -1 (pure torsion), -0.5 (uiniaxial tension), 0(plane strain) and 1 (equibiaxial tension) with von Mises strain range of 0.5% and 1.0% were employed. Nonproportional loading tests, in which 90° phase difference exists between x and y directional strains, were also performed with Mises strain range of 0.5% and 1.0%. Strain path of the nonproportional loading is shown by broken line in Fig.5. Strain rate of all tests was 0.1%/sec for von Mises strain. Fatigue failure life was defined as the number of cycles when either x or y directional load reduced 5% from its maximum value. Test conditions and results are summarized in table 2.

Test Results and Discussion

Cyclic deformation property

The 316FR steel shows cyclic hardening behavior at initial stage and then maintains constant load amplitude until rapid decreasing by cracking. Load-strain hysteresis loops obtained at near mid-life are shown in Fig.6. Coincidence of loops in x-and y-direction in ϕ = 1 and -1 confirms that the biaxial tests by using the new developed machine are reliably performed. In the proportional loading tests for the same Mises strain range, y directional peak load is the largest in ϕ = 0 and smallest in ϕ = -1. In the 90° phase difference nonproportional loading tests, although the y-directional peak load is almost the same as that in ϕ = 0, the peak load in x-direction is larger than that in y-direction in spite of the same strain range. In the y directional loops in proportional loading tests, it can be seen that slope ratio of load to strain both

Table 1 Chemical composition

wt(%)

C	Si	Mn	P	S	Ni	Cr	Co	N
0.008	0.53	0.85	0.026	0.004	11.16	16.88	0.07	0.0754

Table 2 Biaxial fatigue test conditions and results

ϕ	Δεm (%)	strain range y (%)	strain range x (%)	Load range y (kN)	Load range x (kN)	Failure life Nf (cycles)
1	1.0	0.5	0.5	112.8	114.4	4572
	0.5	0.25	0.25	83.6	84.8	123806
0	1.0	0.87	0	112.8	79.8	1420
	0.5	0.44	0	101.5	65.8	49227
-0.5	1.0	1.0	0.52	94.4	0	3046
-1	1.0	0.87	0.87	52.3	57.2	10256
	0.5	0.44	0.44	42.6	45.2	>170000
Non-proportional	1.0	0.87	0.87	125.7	149.6	816
	0.5	0.44	0.44	104.2	110.9	8630

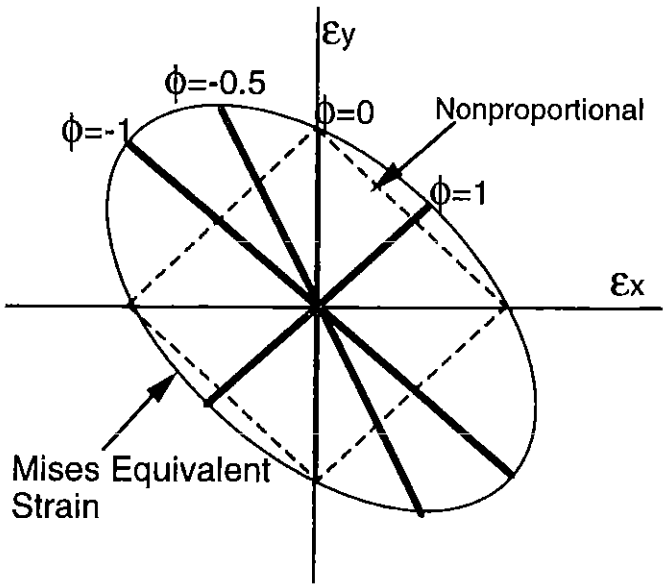

Fig.5 Strain path of proportional and nonproportional tests

at just after passing minimum strain and at before reaching maximum strain, which are equivalent to the elastic modules and hardening coefficient respectively, became larger with increasing the principal strain ratio. In Fig. 6(e), numbers designated in the strain waveforms of nonproportional loading, where x directional strain is 90° ahead of y directional strain, are corresponding to the numbers in the loops. Shape of the loops is different from that in proportional loading and different between x and y directions. The slope ratio of load to strain is relatively small when x and y directional strains go to reverse direction such as 1-2 and 3-4 periods, whereas it takes relatively large value when direction of x and y directional strain is coincident such as 2-3 and 4-1 in the strain waveform. Thus the loops in nonproportional loading produced incontinuous shapes relating to change in strain going direction between x and y directional strain.

Failure appearance

Macroscopic appearances of specimen surface and failure surfaces at the middle of specimen thickness observed by a scanning electron microscope are shown in Fig.7. Since maincracks propagated within the gage area, validity of the specimen design was experimentally verified. Macrocracks propagated only in the x-direction in $\phi = 0$ and -0.5 and both in the x and y directions in $\phi = 1$. The maicrocracks initiated both in the x- direction and the maximum shear direction, and connected with each other in $\phi = 0$. These failure appearances might be expected based on the applied strain conditions. The maincrack propagated only in the y direction in the nonproportional loading where the maximum load amplitude occurred in the x direction. Clear striations indicating that the crack propagated mainly under the Mode I loading, are observed in all failure specimens both under proportional and nonproportional loading. In $\phi = 1$, a secondary cracks initiated in the normal direction to the failure surface due to contribution by x-directional applied strain. Fractography of $\phi = -1$ is the failure surface normal to the y axis. Significant difference of failure surfaces was not identified.

Fatigue life property

Comparison between fatigue failure lives under proportional loading for the same Mises equivalent strain range is shown in Fig.8. Failure life depends on principal strain ratio showing the shortest life in $\phi = 0$ and the longest in $\phi = -1$. Correlation between fatigue failure life and Mises equivalent strain range was shown in Fig.9. Fatigue life data is widely scattered depending on ϕ and loading mode. Fatigue life under nonproportional loading is shorter than

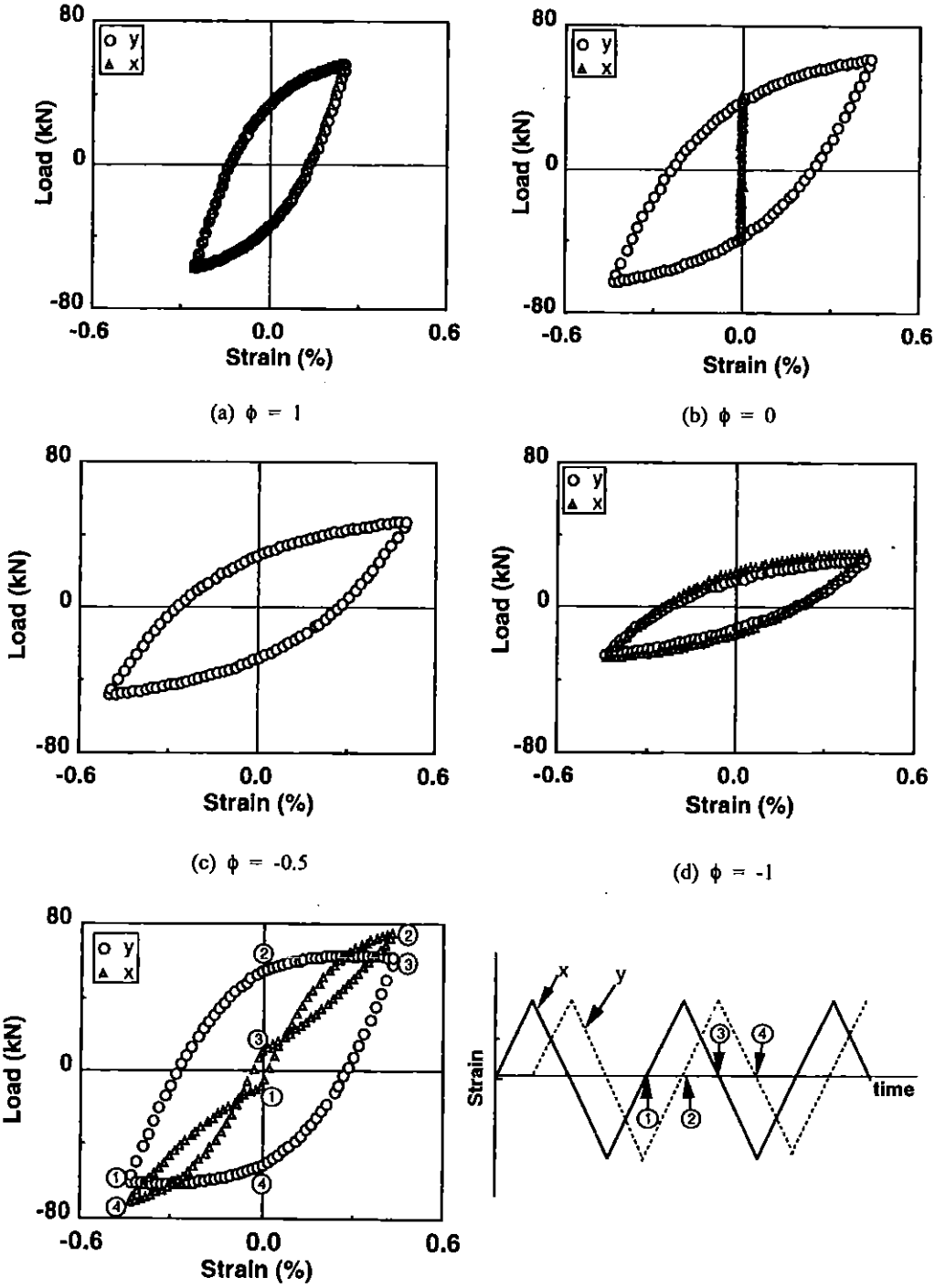

Fig.6 Load-strain hysteresis loop in proportional and nonproportional loading

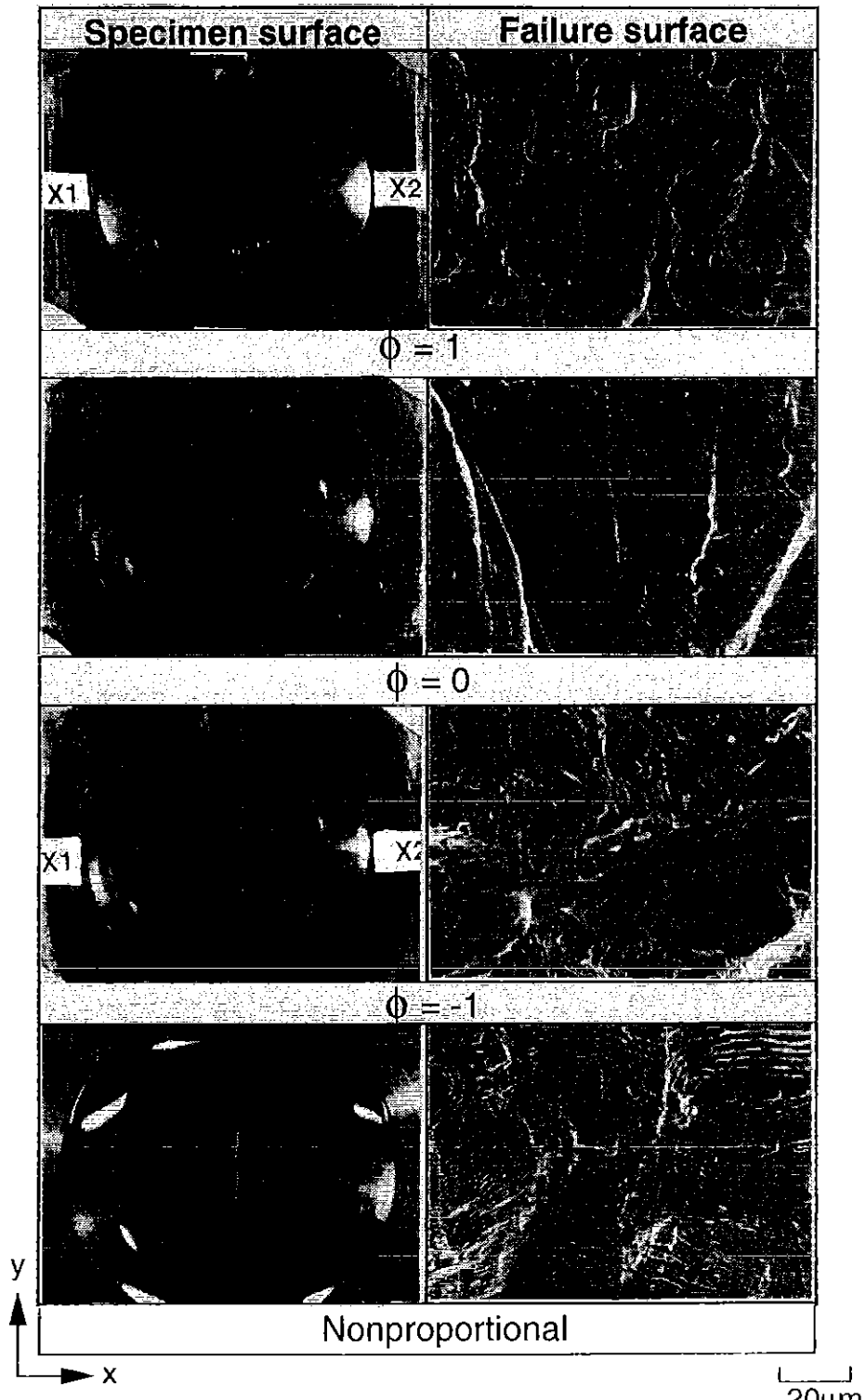

Fig.7 Macrocracks on the specimen surface and fractography

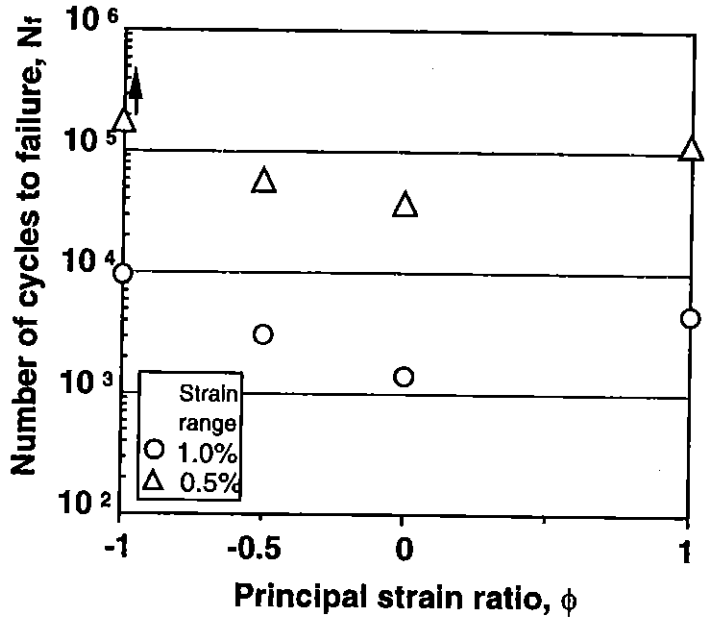

Fig. 8 Dependency of biaxial fatigue life on principal strain ratio

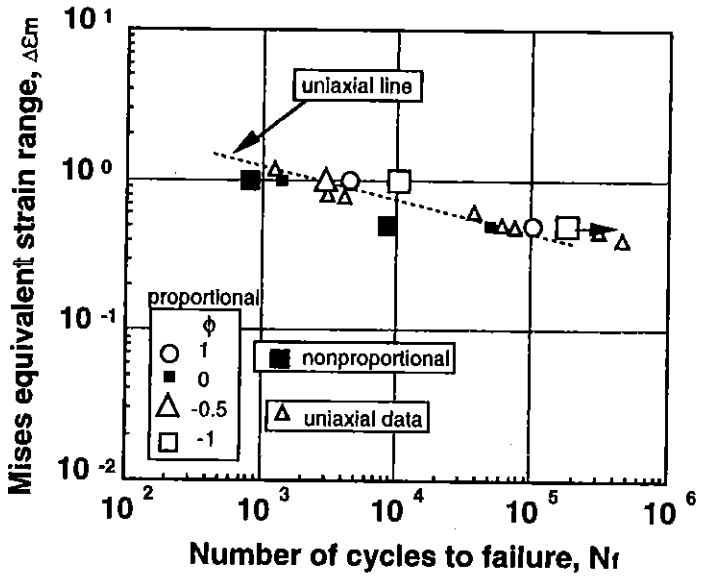

Fig. 9 Relation between Mises equivalent strain range and biaxial fatigue life

that under proportional loading. This means that life prediction for nonproportional loading by Mises equivalent strain range based on uniaxial data gives unconservative prediction.

New biaxial fatigue life criterion

From the design point of view, development of a biaxial fatigue criterion, which can correlate biaxial fatigue life data with uniaxial data, is important to predict failure life of components subjected to biaxial stress. The authors performed tension/compression and torsion tests under proportional and nonproportional loading conditions and fatigue failure criterion , equivalent shear strain range $\Delta\gamma_u$, was previously proposed based on experimental results and strain analysis(2). Biaxial fatigue criterion for proportional loading, where principal strain axis is fixed during a cycle, and nonproportional loading, where principal strain axis rotates during a cycle, are expressed as follows:

$$\overline{\Delta\gamma}_u=\frac{1}{U}\left\{(\Delta\gamma_{max}/2)^2+12.0\Delta\varepsilon_n^2\right\}^{1/2} \quad \text{(proportional)} \qquad (1)$$

$$\overline{\Delta\gamma}_u=\frac{1}{U}(\Delta\gamma_{max}/2+1.2\Delta\varepsilon_n) \quad \text{(nonproportional)} \qquad (2)$$

$$U=1\left\{\left(\frac{1+\nu}{2}\right)^2+12.0\left(\frac{1-\nu}{2}\right)^2\right\}^{1/2} \qquad (3)$$

where $\Delta\gamma_{max}$ is the maximum range of shear strain, $\Delta\varepsilon_n$ is range of normal strain on the $\Delta\gamma_{max}$ plane and ν is Poisson's ratio. Biaxial fatigue lives both under proportional and nonproportional loading correlated well with $\Delta\gamma_u$.

In this study, a unified criterion for the whole range of biaxial stress state under proportional loading is considered. Relationship between failure life and $\Delta\varepsilon_y$ is shown in Fig.10. It is seen that failure life is not controlled by only the maximum principal strain range but affected by $\Delta\varepsilon_x$. Based on the experimental results, fatigue failure life criterion can be drawn on ε_x- ε_y plane as a diamond shape shown in Fig.11, where ν is assumed to be 0.5 and an elliptical shape drawn by broken line represents the Mises equivalent strain criterion. According to the new criterion, equivalent normal strain range $\Delta\varepsilon_u$ is simply expressed by:

$$\Delta\varepsilon_u=\frac{1}{1+A\nu}\Delta\varepsilon_y-\frac{A}{1+A\nu}sig(\phi)\Delta\varepsilon_x \qquad (4)$$

where A is a material constant and determined as 0.38 from Fig.11. Although the new crite-

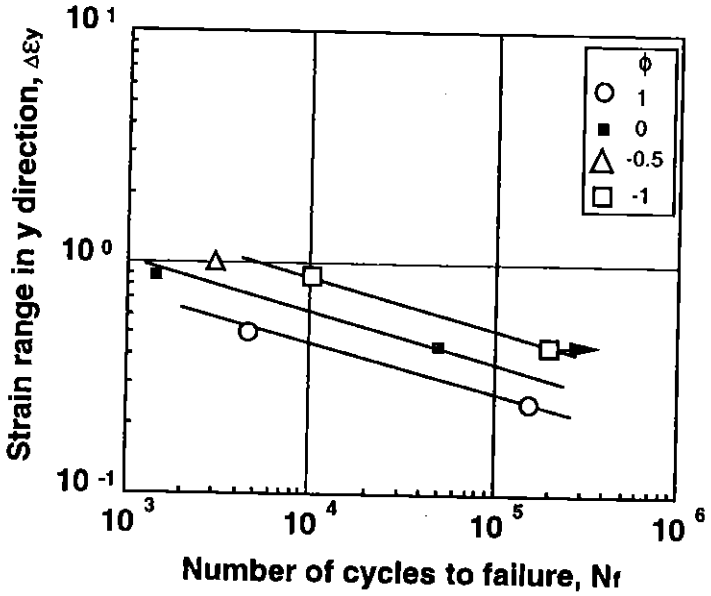

Fig. 10 Relationship between principal strain range and biaxial fatigue life

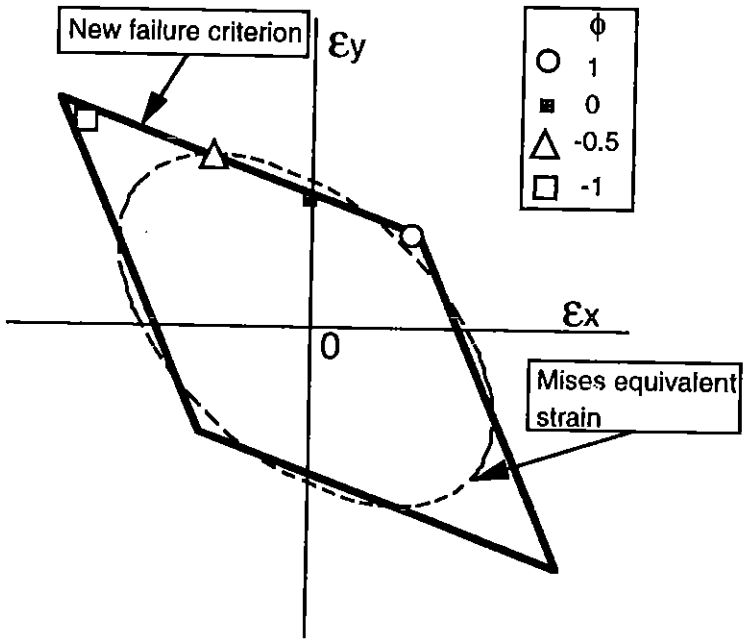

Fig. 11 New biaxial fatigue life criterion on εx - εy diagram

rion gives slightly different results in comparison with theprediction by equation(1), it can be applied to the whole range of biaxial stress state under proportional loading. Previously obtained biaxial fatigue data by tension/compression and torsion tests on 304 stainless steel are correlated with $\Delta\varepsilon_u$ in Fig.12. A broken line represents a best fit curve of fatigue data obtained from uniaxial tests(6). Good correlation can be seen between $\Delta\varepsilon_u$ and fatigue life without dependence on principal strain ratio.

The failure life under 90° phase difference nonproportional loading was shorter than that in $\phi = 0$ in spite of the same $\Delta\varepsilon_y$. This fact also suggests that $\Delta\varepsilon_x$ should be taken into account for the criterion of nonproportional loading. Since ϕ varies during a cycle under nonproportional loading, definition of $\Delta\varepsilon_x$ and its signal were considered based on shape of the new fatigue criterion and strain path of nonproportional loading in Fig.11. Then $\Delta\varepsilon_x$ was defined as a range of the maximum strain in the x direction during a cycle, and the sign is positive when ϕ at the maximum strain in y direction is between 0 and 1, and the sig(ϕ) in equation (4) is replaced by ϕ when ϕ is smaller than 0. Correlation of biaxial fatigue lives of the 316FR stainless steel under proportional and nonproportional loading with $\Delta\varepsilon_u$ is shown in Fig.13. Uniaxial testing data obtained in the CRIEPI is also incorporated. It can be seen that biaxial fatigue lives correlated well with $\Delta\varepsilon_u$ regardless of strain ratio and loading mode. It can be thus concluded that $\Delta\varepsilon_u$ is a useful criterion to predict fatigue failure life of actual components subjected to proportional or nonproportional loading.

Conclusions

A high-temperature biaxial fatigue testing machine(HTBFM) using a cruciform specimen was developed and biaxial fatigue tests were performed on 316FR stainless steel at 550°C. The main results obtained in this study are summarized as follows.

1. Biaxial fatigue tests under proportional and nonproportional tests were successfully performed by the HTBFM using a cruciform specimen which was designed by 3D finite element analysis.

2. It was found that biaxial fatigue life could not be correlated with Mises equivalent strain or principal strain range which provides fatigue life under nonproportional loading shorter than

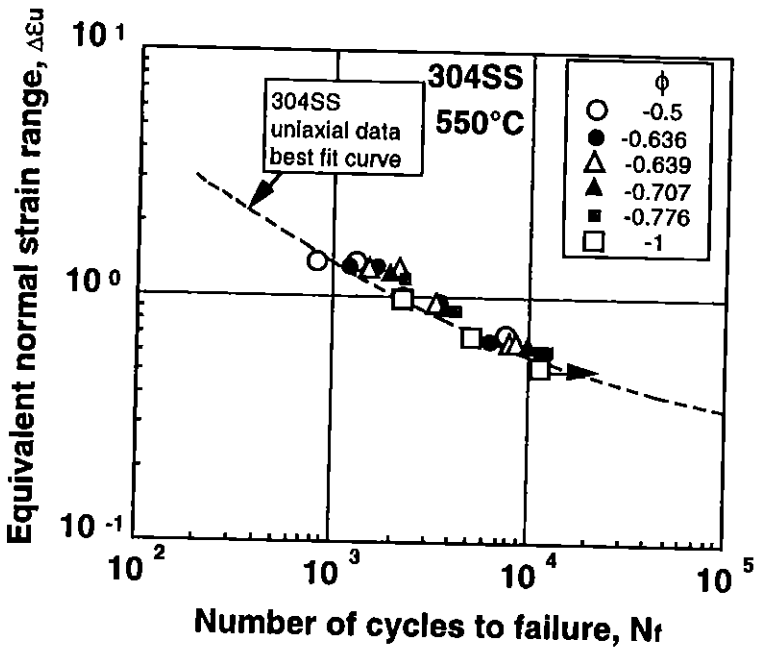

Fig. 12 Correlation of fatigue life of 304 stainless steel with equivalent normal strain range

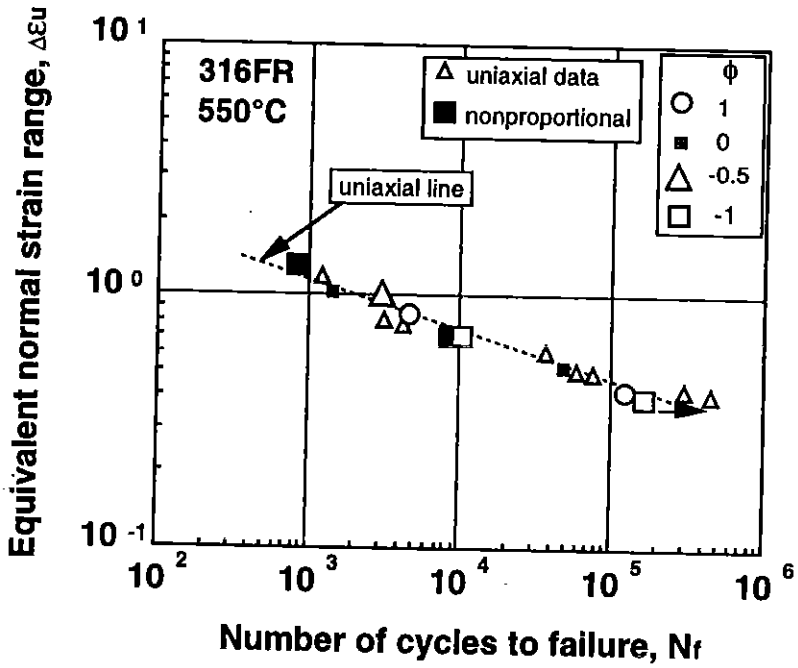

Fig. 13 Correlation of fatigue life of 316FR with equivalent normal strain range

that under proportional loading.

3. Equivalent normal strain range, $\Delta\varepsilon_u$ was proposed as a new biaxial fatigue criterion based on iso-failure line on the applied principal strain diagram. Biaxial fatigue lives both under proportional and nonproportional loading correlated well with $\Delta\varepsilon_u$.

References

(1) Nitta, A., Ogata, T. and Kuwabara, K., (1989), "Fracture Mechanism and Life Assessment under High-Strain Biaxial Cyclic Loading of Type 304 Stainless Steel", Fatigue Fract. Engng. Mater. Struct., Vol.12, No.2, pp.77-92

(2)Ogata, T., Nitta, A. and Kuwabara, K.,(1991), "Biaxial Low-Cycle Fatigue Failure of Type 304 Stainless Steel under In-phase and Out-of-phase Straining Conditions", "Fatigue under Biaxial and Multiaxial Loading", ESIS Publication 10MEP, pp.377-392.

(3)Ogata, T., Nitta, A. and Blass, J. J., (1993), "Propagation Behavior of Small Cracks in 304 Stainless Steel Under Biaxial Low-Cycle Fatigue at Elevated Temperature", *Advances in Multiaxial Fatigue, ASTM STP 1911*, D. L. McDowell and R. Ellis, Eds, pp.313-325.

(4)Sakane, M. and Ohnami, M., (1991), "Creep-Fatigue in Biaxial Stress States using Cruciform Specimen", same as ref.(2), pp.265-278.

(5)Itoh, T., Sakane, M., Ohnami, M., Takahashi, Y. and Ogata, T., (1992), "Nonproportional Multiaxial Low Cycle Fatigue Using Cruciform Specimen at Elevated Temperature", Proc. of 5th Inter. Conf. on Creep Materials, pp.331-339.

(6)Wada, Y., Kawakami, Y. and Aoto, K., (1987), "A Statistical Approach to Fatigue Life Prediction for SUS304,316 and 321 Austenitic Stainless Steels" , ASME Pres. Ves. & Piping, Vol.123, pp.37-42.

Acknowledgments

The authors would like to express our gratitude to staffs of MTS Corporation who made tremendous effort to design, manufacture and install the new machine which meets the provided specification. The work has been conducted within a program sponsored by the Ministry of International Trade and Industry in Japan.